

# Non-enzymatic glucose biosensor based on reduction graphene oxide-persimmon tannin-Pt-Pd nanocomposite

Yewei Xue, Yong Huang, Zhide Zhou\*, Guiyin Li\*

School of Life and Environmental Sciences, Guilin University of Electronic Technology, Guilin, Guangxi 541004, China

E-mail: 18291455419@163.com (Y.W.Xue); \*liguiyin01@163.com (G.Y. Li); \*zzdlgy@126.com (Z.D.Zhou)

**Abstract:** Herein, a novel non-enzymatic glucose sensor was fabricated based on the reduction graphene oxide-persimmon tannin-platinum-palladium alloy (RGO-PT-Pt-Pd) nanocomposite. The RGO-PT-Pt-Pd nanocomposite was prepared through a facile approach with PT as film material and ascorbic acid as reducing agent and characterized by ultraviolet visible spectroscopy (UV-vis), Fourier transform infrared spectroscopy (FT-IR), Scanning electron microscopy (SEM), X-Ray diffraction (XRD) and so on. Then, the synthesized RGO-PT-Pt-Pd nanocomposite was employed as an electrode material for non-enzymatic glucose sensing using gold electrode (GE). The RGO-PT-Pt-Pd/GE sensor showed outstanding catalytic activity toward glucose oxidation. The prepared amperometric sensor exhibited a wide linear range of 0.01-0.40 mol/L with a limit of detection (1.43  $\mu\text{mol/L}$ ) as well as high stability and fast responsetime (<3s). Therefore, the glucose biosensor has the potential to be used for clinical blood glucose detection.

## 1. Introduction

Diabetes is regarded as one of the most important global health problems characterized by an escalation in blood sugar levels (hyperglycemia) which results in an enhanced risk of serious illnesses such as stroke, obesity, kidney failure and coronary heart disease [1-3]. Sensitive detection of abnormal glucose levels in the blood is momentous in order to properly treat and reduce many health problems [4, 5]. Among many different technologies for detecting glucose, electrochemical sensors are considered to be the most successful protocol for glucose testing so far [6]. In recent years, a large number of electrode materials have been exploited to improve the electrocatalytic activity of glucose [7, 8]. Many stable, specific, and cost-effective biosensors using different nanomaterials have been reported with the advancement of nanotechnology. However, it is regrettable that the key technology research can't appease the demand of the market in particular for glucose sensor [9]. Reduced graphene oxide (RGO), which has the characteristics of a monolayer densely packed with carbon atoms in two-dimensional honeycomb (2D) lattices, also has unique electronic, physical, mechanical and chemical properties and is therefore widely used in physics and chemistry [10]. Nevertheless, the intense intermolecular  $\pi$ - $\pi$  laminating, RGO incline to agglomerate and sandwich, thus affecting its dispersion [11]. Persimmon tannin (PT), a water-soluble and low-cost natural biopolymer, could adsorb onto the surface of RGO surface through  $\pi$ - $\pi$  and electrostatic interactions to prevent aggregation for better stability [12,13]. Most significant, noble metal nanoparticles exhibit excellent electrocatalytic activity for glucose redox reactions especially Pt, Pd NPs [2,8,14].

In the paper, a newfashioned non-enzymatic biosensor derived from the RGO-PT-Pt-Pd



nanocomposite was introduced to take a detection test for glucose. The RGO-PT-Pt-Pd nanocomposite was prepared through a facile approach with PT as film material and ascorbic acid as reducing agent. The synthesized nanocomposite was employed as an electrode material for non-enzymatic glucose sensing using gold electrode (GE). Availing oneself of the fine electro-catalytic productivity of Pt-Pd NPs, high electroconductibility of RGO and good biocompatibility of PT, the integration of each material also brought together the advantages of each material and achieved great properties through synergistic action. The RGO-PT-Pt-Pd sensor showed outstanding catalytic activity toward glucose reduction.

## 2. Experimental

### 2.1 Reagents

Graphene-oxide (GO) was bought from TIMENANO Company (Chengdu, China). Persimmon tannin (the feed material extracted from astringent persimmon) was harmoniously provided by Guangxi Huikun Company of Agricultural Products (Guangxi, China). Chloroplatinic acid ( $\text{H}_2\text{PtCl}_6$ ), palladium nitrate ( $\text{Pd}(\text{NO}_3)_2$ ) and ascorbic acid (AA) were obtained from Sinopharm Chemical Reagent Co., Ltd (Tianjin, China). The other reagents were of analytical grade and can be used without further purification. All water mentioned throughout the experiment was designated 18 M $\Omega$  cm Millipore ultrapure water.

### 2.2 Apparatus

Electrochemical measurements were implemented on CHI660 electrochemical workstation (ChenHua Instrument, Shanghai, China). A traditional three electrode system included a gold electrode (GE, 3.0 mm diameters) as the working initial electrode, a platinum wire was used as auxiliary electrode, and a saturated calomel electrode (SCE) was exploited as reference electrode. Amperometric *i-t* curve (*i-t*), Cyclic voltammetry (CV) was performed in 0.1 M phosphate buffer (PBS, including 0.1 mol/L NaCl, pH 7.4).

The morphology and structure of the RGO-PT-Pt-Pd nanocomposite were characterized by ultraviolet visible spectroscopy (UV-vis, UH5300, HITACHI, Japan), Fourier transform infrared spectroscopy (FT-IR, Bruker Tensor 27, Germany), Scanning electron microscopy (SEM, Quanta 200, Elementar, Germany), X-Ray diffraction (XRD, D8 Advance, Germany).

### 2.3 Preparation of the RGO-PT-Pt-Pd nanocomposite

RGO-PT-Pt-Pd nanocomposite was synthesized through a facile approach with PT as film-forming material. Firstly, 10 mL 0.1 mg/mL of GO was vigorous stirring with ultrasonic for 2 h to form a uniform suspension, then 10 mg AA was slowly added and stirred for 12 h to attain RGO. Next, 20 mg PT was affiliated 10 mL 0.1 mg/ml RGO liquid with the ultrasonic dispersion about 90 mins to gain uniformly well-distributed RGO-PT suspension. Lastly, 2 mL 0.01 g/mL  $\text{H}_2\text{PtCl}_4$  and 2 mL 0.05 g/mL  $\text{Pd}(\text{NO}_3)_2$  solutions were added into RGO-PT suspension and AA was tardily added before vigorous agitated 20 h, following by the mixed solution was centrifuged for 15 min at 10000 rpm, removed the supernatant, washed thrice with ultrapure water and got the RGO-PT-Pt-Pd., and then stored in refrigerator at 4 °C after drying.

### 2.4 Preparation of the glucose biosensor on RGO-PT-Pt-Pd nano-composites basis

Gold electrode was polished sequentially with 0.3 and 0.05 mm  $\text{Al}_2\text{O}_3$  powder, sonicated for 5 min each in ethanol and ultrapure water. After washed well with 0.1 M PBS, 5  $\mu\text{L}$  0.1 mg/mL RGO-PT-Pt-Pd solution was pipetted onto the polished gold electrode surface and dried at room temperature. After dropped RGO-PT-Pt-Pd solution for 3 times, a nonenzymatic glucose biosensor based on the RGO-PT-Pt-Pd nanocomposite was fabricated.

### 2.5 Electrochemical detection of glucose with RGO-PT-Pt-Pd/GE non-enzymatic biosensor

During the measurement, different concentrations of glucose was continuously added to PBS (0.1M, pH 7.4, including 0.1M NaCl) solution, and the generated electrochemical signals were recorded by amperometric i-t technology at a voltage of -0.3 V while the solution was stirred by a magnetic stirrer (speed about 100 rpm).

## 3. Results and discussion

### 3.1 Characterization of RGO-PT-Pt-Pd nanocomposites

FT-IR spectroscopy was implemented investigation to investigate the possible interactions between the nanocomposite. Fig. 1(A) showed the FT-IR spectra of GO (curve a), RGO-PT (curve b) and RGO-Pt-Pd NPs (curve c). The peak at  $1718\text{ cm}^{-1}$  and at  $1120\text{ cm}^{-1}$  were attributed to the C=O stretching vibration and the C-O-C absorption vibration from the oxygen group of GO, respectively (curve a). Correspondingly, FT-IR spectra of the RGO-PT-Pt-Pd NPs (curve c) showed that the  $1120\text{ cm}^{-1}$ ,  $1718\text{ cm}^{-1}$  original absorbance peak was evidently weakened, most of all the C-O expansion vibration peak of graphene completely disappeared at  $1718\text{ cm}^{-1}$ .

Further reduction of  $\text{Pt}^{2+}$ ,  $\text{Pd}^{2+}$  to graphene surface was confirmed by UV-visible absorption spectrum Fig. 1(B). By comparing the GO (curve a) with the RGO-PT-Pt-Pd NPs (curve b), there is a wider peak completely disappeared in the RGO-PT-Pt-Pd solution after adding the reducing agent ascorbic acid at 304 nm which the  $n \rightarrow \pi^*$  transition of the C=O double bond, and the characteristic absorption peak of  $\text{H}_2\text{PtCl}_6$  was not found at 258 nm, indicated that most of the oxygen-containing group had been reduced on the surface of the graphene and the  $\text{Pt}^{2+}$  in solution was reduced to the surface of the graphene by the reducing agent ascorbic acid.

The crystalline structure of the material was effectively analyzed by XRD diffraction instrument. As shown in Fig. 1(C), it was the XRD diffraction spectrum of RGO-PT-Pt-Pd NPs. The diffraction peak of  $2\theta = 24.9^\circ$  corresponded to the graphene C (002) crystal plane. The diffraction peaks at  $2\theta = 39.7^\circ$ ,  $46.1^\circ$  and  $67.4^\circ$  corresponded to the (111), (200) and (220) planes of Pt and Pd NPs, respectively. Since Pt and Pd NPs were geared to the same family, thus had the same crystal structure. It can be seen from the diagram that the peaks of C (002) were stronger, while the peak value of the diffraction peak of Pt and Pd NPs were weaker. It can be confirmed that the Pt and Pd NPs had been adsorbed on the surface of graphene and the diffraction peak sharper, indicated that the better degree of crystallization.

The appearance of the RGO-PT-Pt-Pd nanocomposite was characterized by SEM in Fig. 1(D). There was portrait distinctly found that the film was wrapped with numerous bright white particles, which film was RGO-PT composite, particles of Pt, Pd NPs and the size of particles about 100 nm. All in all, RGO-PT-Pt-Pd nanocomposite was successfully synthesized.

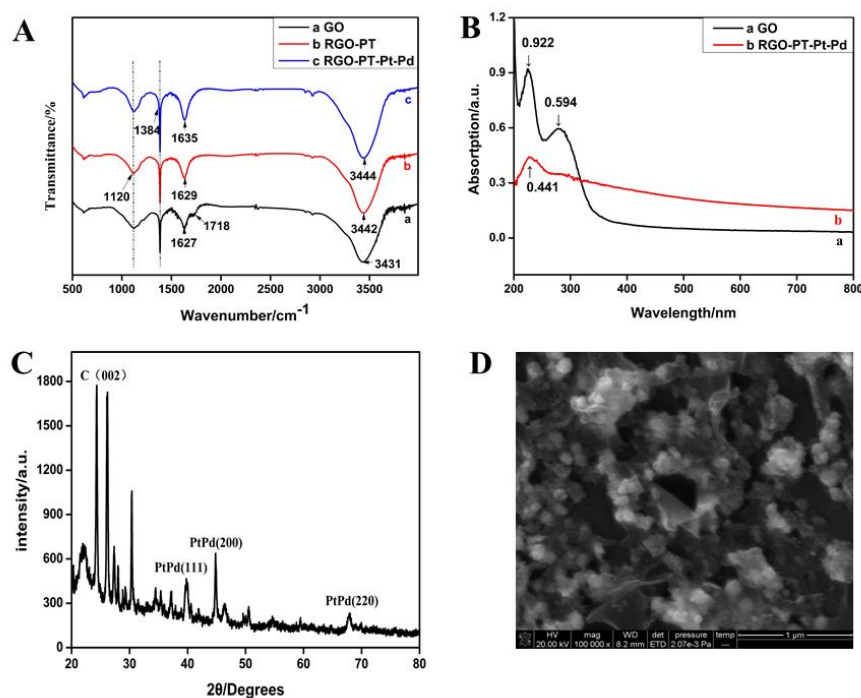


Fig.1 FT-IR spectra for GO, RGO-PT, RGO-PT-Pt-Pd NPs (A); UV-visible spectrum for GO, RGO-PT-Pt-Pd NPs (B); XRD spectrum for RGO-PT-Pt-Pd NPs (C); SEM image for RGO-PT-Pt-Pd NPs(D)

### 3.2 Principle analysis of the glucose biosensor on RGO-PT-Pt-Pd nanocomposite basis

Fig.2 illustrated the analytical principle of the prepared biosensor for glucose detection. First, RGO-PT-Pt-Pd nano-composites were prepared through a facile approach with PT as film material and ascorbic acid as reducing agent. Then, the RGO-PT-Pt-Pd nanocomposite was immobilized onto surface of the pretreated gold electrode via electrostatic adsorption. Electrons generated during the electrocatalytic decomposition of glucose by Pt-Pd NPs were quickly transferred to the gold electrode in order to produce a sensitive glucose quantitation current. The RGO-PT-Pt-Pd nano-composites showed good catalysis activities through a synergistic effect Avail oneself of the fine electro-catalytic productivity of Pt-Pd NPs, preminent electroconductibility of RGO and good biocompatibility and film forming ability of PT. To the best of our knowledge, this is the fabulous application of RGO-PT-Pt-Pd nanocomposites for glucose detection.

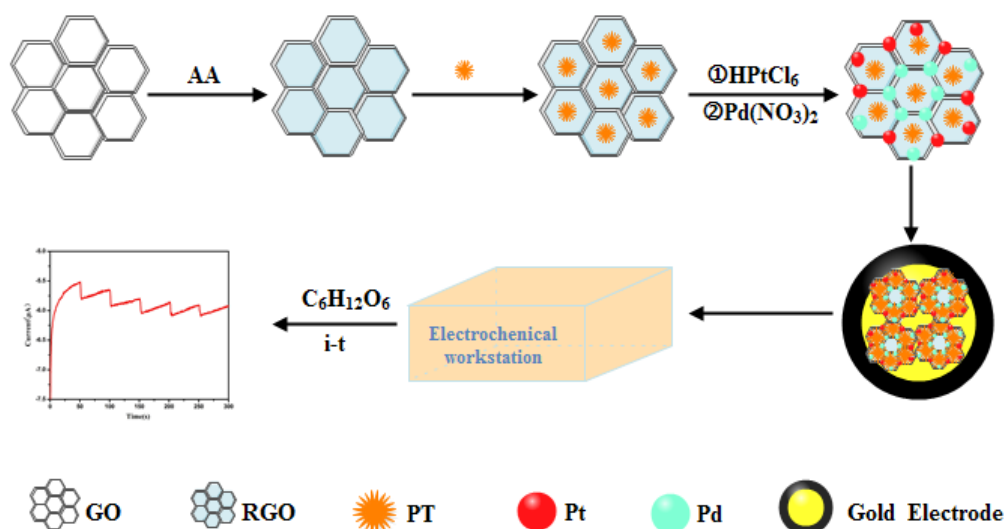


Fig.2 Principle of biosensor detection for glucose

### 3.3 Linear dynamic range

The non-enzymatic electrochemical biosensor on RGO-PT-Pt-Pd nano-composites basis to accelerate the oxidation of glucose and gauge the oxidation current which was obtained through *i-t* technology at a certain potential. Fig.3A showed the amperometric response of RGO-PT-Pt-Pd/GE to glucose catalytic breakdown at a potentiostatic potential of -0.3V, serially added to 0.1 M PBS (5 additions) at 50s intervals. The electrode rapidly reacted after glucose was added, reached 95% of the steady-state current for less than 2 s (illustration in Fig.3A), indicated an extremely rapid and hypersensitive response to glucose. The calibration curve for a non-enzymatic electrochemical biosensor was shown in Fig. 3B. the response current was linear with the concentration of glucose over the range 0.01-0.4mol/L. The linear regression equation was  $y = 1.3046x - 0.00186$  ( $y$  was the sensor response current value,  $x$  was the glucose concentration), and the regression correlation index coefficient was 0.99873. It can be inferred that the linearity of glucose biosensor was very great and the minimum detection limit was reached  $1.43 \mu\text{mol/L}$  ( $S/N = 3$ ). The proposed glucose biosensor possessed rapid response speed, hypersensitive, the potential detection of the glucose biosensor also had a good reproducibility.

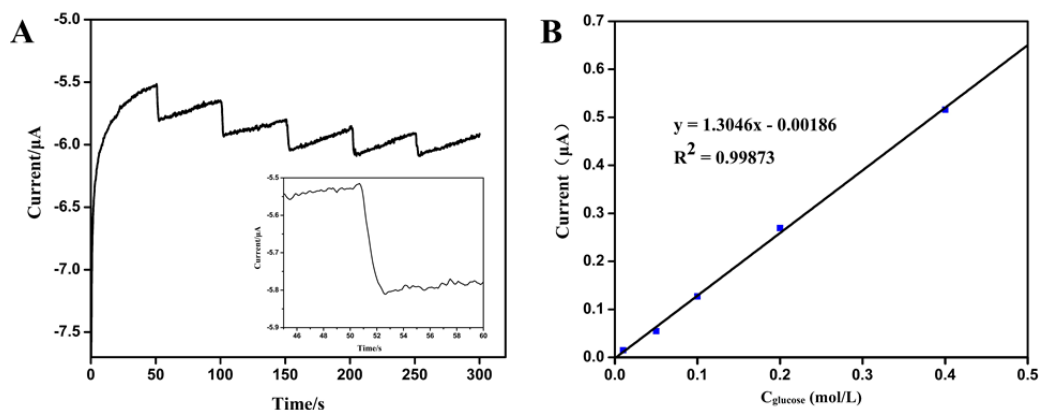


Fig.3 Standard curve for determination of glucose

## 4. Conclusion

On balance, a novel glucose biosensor was developed based on RGO-PT-Pt-Pd/GE. The RGO-PT-Pt-Pd nanocomposite were synthesized through direct reduction of AA reduction. Based on

the satisfactory biocompatibility and electron transfer ability of RGO-PT nanohybrids and the satisfactory electro-chemical catalysis capabilities of Pt-Pd NPs, the non-enzymatic glucose biosensor displayed a linear dynamic current in reliance upon the glucose concentrations over the range 0.01-0.4 mol/L with a readily achievable detection limit of 1.43  $\mu\text{mol/L}$  and the response time of 2 s. This novel glucose biosensor can be very useful and provide favorable application promises in providing a potent, specific, and sensitive method to detect plasma glucose.

### Acknowledgments

This work was supported by the National Nature Science Foundation of China (Nos. 81372362, 81460451, 81760534 and 81430055), Guangxi key industry science and technology innovation project (No.1598005-3), the Innovation Project of GUET Graduate Education (Nos.YCSW2017146 and 2017YJXC95), and the National Science Foundation of Guangxi province of China (Nos. 2016GXNSFAA380011 and 2016GXNSFAA380080)

### References

- [1] Atta NF, Galal A, El-Ads EH. Electrochemistry of glucose at gold nanoparticles modified graphite/SrPdO<sub>3</sub> electrode towards a novel non-enzymatic glucose sensor [J]. *Journal of Electroanalytical Chemistry*, 2015, 749:42-52.
- [2] Chen X, Pan H, Liu H, Du M. Nonenzymatic glucose sensor based on flower-shaped Au@Pd core-shell nanoparticles ionic liquids composite film modified glassy carbon electrodes [J]. *Electrochimica Acta*, 2011, 56(2):636-643.
- [3] Steele JA, Hallé JP, Poncelet D, Neufeld RJ. Therapeutic cell encapsulation techniques and applications in diabetes [J]. *Advanced Drug Delivery Reviews*, 2014, 67-68(1):74-83.
- [4] Choudhary M, Shukla SK, Taher A, Siwal S, Mallick K. Organic-inorganic hybrid supramolecular assembly: An efficient platform for nonenzymatic glucose sensor [J]. *ACS Sustainable Chemistry and Engineering*, 2014, 2 (12):2852 -2858.
- [5] Zhang P, Zhao X, Ji Y, Qu Y, Wen X, Li J, Su Z, Wei G. Electrospinning graphene quantum dots into a nanofibrous membrane for dual-purpose fluorescent and electrochemical biosensors [J]. *Journal of Materials Chemistry B*, 2015, 3(12):2487-2496.
- [6] Zhai Y, Li J, Chu X, Xu Z, Jin F, Li X, Fang X, Wei Z, Wang X. MoS<sub>2</sub> microflowers based electrochemical sensing platform for non-enzymatic glucose detection [J]. *Journal of Alloys and Compounds*, 2016, 672:600-608.
- [7] Zhang J, Xu C, Zhang R, Guo X, Wang J, Zhang X, Zhang D, Yuan B. Solvothermal synthesis of cobalt tungstate microrings for enhanced nonenzymatic glucose sensor [J]. *Materials Letters*, 2018, 210:291-294.
- [8] Tang Y, Liu Q, Jiang Z, Yang X, Wei M, Zhang M. Nonenzymatic glucose sensor based on icosahedron AuPd@CuO core shell nanoparticles and MWCNT [J]. *Sensors and Actuators B Chemical*, 2017, 251:1096-1103.
- [9] Hsu CL, Fang YJ, Hsueh TJ, Wang SH, Chang SJ. Nonenzymatic glucose sensor based on Au/ZnO core-shell nanostructures decorated with Au nanoparticles and enhanced with blue and green light[J]. *Journal of Physical Chemistry B*, 2017, 121(14): 2931-2941.
- [10] Rummeli MH, Rocha CG, Ortman F, Ortman F, Ibrahim I, Sevincli H, Börrnert F, Kunstmann J, Bachmatiuk A, Pötschke M, Shiraishi M, Meyyappan M, Büchner B, Roche S, Cuniberti G. Graphene: Piecing it together [J]. *Advanced Materials*, 2011, 23(39):4471-4490.
- [11] Yin H, Zhou Y, Ma Q, Ai S, Ju P, Zhu L, Lu L. Electrochemical oxidation behavior of guanine and adenine on graphene-Nafion composite film modified glassy carbon electrode and the simultaneous determination [J]. *Process Biochemistry*, 2010, 45(10):1707-1712.
- [12] Wang Z, Li X, Liang H, Ning J, Zhou Z, Li G. Equilibrium, kinetics and mechanism of Au<sup>3+</sup>, Pd<sup>2+</sup> and Ag<sup>+</sup> ions adsorption from aqueous solutions by graphene oxide functionalized persimmon tannin [J]. *Materials Science and Engineering C*, 2017, 79:227-236.
- [13] Zheng Y, Wang A, Wai W, Wang Z, Peng F, Liu Z, Fu L. Hydrothermal preparation of reduced

- graphene oxide–silver nanocomposite using *Plectranthus amboinicus*, leaf extract and its electrochemical performance [J]. *Enzyme and Microbial Technology*, 2016, 95:112-117.
- [14] Yang C, Cui X, Wang K, Cao Y, Wang C, Hu X. A Non-Enzymatic Glucose Sensor Based on Pd-Fe/Ti Nanocomposites[J]. *International Journal of Electrochemical Science*, 2017, 12(6):5492-5502.